

## MIT Open Access Articles

*A shield ring enhanced equilateral hexagon distributed multi-needle electrospinning spinneret*

The MIT Faculty has made this article openly available. **Please share** how this access benefits you. Your story matters.

**Citation:** Yang, Ying et al. "A Shield Ring Enhanced Equilateral Hexagon Distributed Multi-needle Electrospinning Spinneret." IEEE Transactions on Dielectrics and Electrical Insulation 17.5 (2010): 1592–1601. © 2010 IEEE.

**As Published:** <http://dx.doi.org/10.1109/TDEI.2010.5595562>

**Publisher:** Institute of Electrical and Electronics Engineers (IEEE)

**Persistent URL:** <http://hdl.handle.net/1721.1/73190>

**Version:** Final published version: final published article, as it appeared in a journal, conference proceedings, or other formally published context

**Terms of Use:** Article is made available in accordance with the publisher's policy and may be subject to US copyright law. Please refer to the publisher's site for terms of use.



# A Shield Ring Enhanced Equilateral Hexagon Distributed Multi-needle Electrospinning Spinneret

Ying Yang, Zhidong Jia, Qiang Li, Lei Hou, Jianan Liu, Liming Wang, Zhicheng Guan

Tsinghua University  
Department of Electrical Engineering,  
Haidian District, Beijing, China, 100084  
Tsinghua University Shenzhen Graduate School  
Laboratory of Advanced Technology of Electrical Engineering & Energy,  
Shenzhen, Guangdong, China, 518055

and **Markus Zahn**

Massachusetts Institute of Technology  
Department of Electrical Engineering and Computer Science  
Research Laboratory of Electronics (RLE)  
Laboratory for Electromagnetic and Electronic Systems (LEES)  
High Voltage Research Laboratory  
77 Massachusetts Avenue  
Cambridge, Massachusetts 02139

## ABSTRACT

The multi-needle electrospinning system is a convenient way to produce fibers with special structures such as core-shell morphologies at a high production rate. In this paper, a specially designed multi-needle electrospinning system is presented. The spinnerets were built-up with an equilateral hexagon array. Each set of 3 needles of the spinnerets were distributed as an equilateral triangle. A coaxial shield ring was used to create an approximate uniform electric field near the tips of the needles and to restrict the collection area. The simulation results also show that the outside needles can help to create a more uniform electric field near the inside tips of the needles and restrict the path of the inside jets, which works almost the same as the additional shield ring. Based on the simulation results, several multi-needle systems were tested. A 7 cm diameter shield ring was used in a 7 needle system, a 9 cm diameter shield ring was used in a 19 needle system and a 10.5 cm diameter shield ring was used in a 37 needle system. Polyethylene Oxide (PEO) aqueous solution was used as the test solution in experiments. The electrospinning results demonstrated that the use of multi-needle spinnerets is robust and that uniform nanofibers can be produced. The more needles used, the smaller the mean fiber diameter for larger mean electric field strengths. These distributions of needles show the scale up possibility of special structure electrospun nanofiber manufacturing.

Index Terms - Multi-needle electrospinning; electric field distribution nanofiber

## 1 INTRODUCTION

**ELECTROSPUN** fibers have recently become an object of intensive experimental research due to potentially broad markets for fibers with diameters as small as 100 nm. Electrospun mats with large surface area have numerous potential applications such as filtration [1], drug delivery [2], and tissue engineering [3].

The flow rate for a single needle setup is typically 0.001-1.0 ml/min. The low production rate of the single needle electrospinning process and the non-uniform fibers produced with the multi-jet spinning process may limit the industrial use

of electrospinning. Although the most common electrospun mat could be produced with a needleless nanospider at a high production rate [4], the multi-needle system still needs study as it is the best way to produce special structure fibers such as core-shell fibers at higher production rate.

The most difficult issues in the multi-needle system are repulsion from the adjacent jets and the non-uniform electric field on each tip of the needle at different positions of the spinneret, which always cause instability problems such as dripping or non-working needles during the electrospinning process.

To improve the production rate by needleless system, Yarin and his group provided a new approach employing a ferromagnetic liquid sub layer that yields about 26 jets/cm<sup>2</sup>,

but the fiber diameters were broader in distribution from 200 nm to 800 nm [4]. Reneker and his group also tried to produce electrospun fibers using a porous tube. The mass production rate from the porous tube was 250 times greater than the production rate from a typical single needle system but the fiber diameter distribution was from a few tens of nanometers to 400 nm [5]. Elmarco's Nanospider™ Technology has developed a free liquid surface electrospinning process and nanofibers can be produced on an industrial scale for a number of applications [6]. Yarin et al reported that spherical electrodes subjected to supercritical electric fields can be used for simultaneous generation of multiple jets, which is of theoretical and practical interest and in relation for needleless electrospinning [7].

To improve the production rate by a multi-needle system, the Yarin and Zussman group demonstrated a 9 needle model in which the 9 jets could be electrospun steadily from separate needles located with a pitch of 1 cm on a square of 4 cm<sup>2</sup> under comparable conditions to the present work [8]. Tomaszewski and Szadkowski compared 3 types of multi-jet electrospinning heads and found that 10 spinning pipes arranged in a circle with a diameter of 50 mm was the best arrangement in their system [9]. Kim et al used a cylindrical electrode to stabilize the 5 jet electrospinning process [10]. Yang et al reported 3 kinds of spinnerets in order to get a stable electrospinning process with 7 needles [11]. Varesano et al. studied several multi-jet electrospinning setups with 2 to 16 needles by evaluating jet-jet repulsion. The needles followed a square distribution. A secondary electrode several mm above the needle tips has been investigated to obtain a reduction of the divergence [12]. The Jayaram group studied the electric field distribution in 2 needle arrangements by using finite element analysis. They reported that the degree of field distortion correlates with the variation in the measured vertical angle of the straight jet portion for different needle spacing but the influence of needle spacing on average jet current and fiber diameter is not highly significant [13].

To collect an electrospun mat in a relatively small area, Deitzel et al [14] demonstrated a control system using 3 power supplies and 8 rings, which could dampen the electrospinning instability. Kim designed an electrospinning process with a cylindrical auxiliary electrode connected to a spinning nozzle to stabilize the initially spun solution with a parallel-plate electrode as a collector to generate an alternating current electric field for controlling the spun jets [10]. Yang et al designed a novel system using a PVC insulator tube to modify the electric field distribution controlling the jet path [15, 16].

In this paper, to efficiently achieve uniform fibers at a high production rate, a hexagon shaped multi-needle spinneret has been implemented. Each set of 3 needles was designed as an equilateral triangle in this system to have a uniform electric field strength near the inner needles and to restrict the paths of the inside jets. An additional shield ring was also used in order to have a more uniform electric field near the tips of the needles and to restrict the collection area. The shield ring diameter was chosen based on the 3D electric field simulations using Ansoft Maxwell software. The electrospinning results with PEO aqueous solution demonstrated that the special design setup can produce uniform nanoscale fibers with a

stable process. Thinner fibers can be produced with more needles at larger average electric field strength.

## 2 THEORETICAL BASIS

### 2.1 NEEDLE DISTRIBUTION

Assuming the equilateral polygon is  $n$ -isogon, the inner angle should be  $(n-2) \times 180/n$ . If we want to expand the isogon cell in a plane, the inner angle should be  $360^\circ/m$ , where  $m, n$  are integers.

$$[(n-2) \times 180] / n = 360 / m \quad (1)$$

Based on equation (1), there are three geometries, equilateral triangle ( $n=3, m=6$ ), square ( $n=4, m=4$ ) and equilateral hexagon ( $n=6, m=3$ ) as shown in Figure 1, that can be expanded endlessly and can form a centrosymmetry structure in a 2-D plane.

Needles per unit area,  $k$ , for the 3 structures were all calculated by

$$k = \left( \frac{1}{m} \times n \right) / S \quad (2)$$

where  $S$  is the area of the isogon.

The results of the calculations showed that  $k_{\text{triangle}} : k_{\text{square}} : k_{\text{hexagon}} = 6 : 3\sqrt{3} : 4$ , so the equilateral triangle structure is the best one to maximize the total amount of needles per unit area in this paper. The following discussions are all based on this structure.

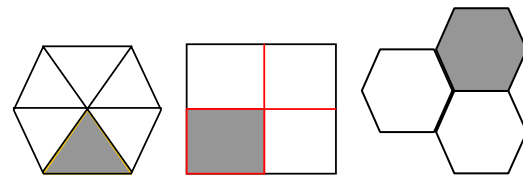


Figure 1. Needle distribution cells.

### 2.2 SHIELD RING

The shield ring has two functional points in this design. One is for collecting the fibers in a smaller area. The other is for forming a uniform electric field near the tips of the needles.

It should be mentioned that the solution flow rate from the pump,  $Q_{in}$  is not exactly equal to the solution flow rate taken away by the electric force  $Q_{out}$ , so that there will be a  $\Delta Q(E, t) = Q_{out} - Q_{in}$ . For each  $Q_{out}$ , there must be an exact electric field strength  $E$ . As the needle distribution will affect the electric field near the tips of the needles in multi-needle systems, the electric field strength  $E$  at each tip of the needle is different from the others. So there is an  $E$  range for each tip of the needle in which the  $\Delta Q$  is too small to form a drop during  $t$  hours.

There are two ways to match the different electric field strengths at the tips of the needles at different positions. One is making the flow rate match the electric field strength at each tip of the needle. The other is improving the uniformity of the electric field at the tips of the needles at different positions of the spinneret. In this paper, we focus on improving the uniformity of the electric field, in other words, to minimize the  $\Delta E$  between each adjacent pair of needles.

In general, the governing equation of the simplest electric field is Poisson's equation for the electric scalar potential  $\varphi$ , given in equation 3

$$\nabla^2 \varphi = -\frac{\rho_f}{\varepsilon} \quad (3)$$

As shown in [18], the calculated total charge on the upper electrode was in the range of  $10^{-10}$ – $10^{-2}$  nC. The total charge on each jet in the space between the two electrodes were in the range of  $10^{-6}$ – $10^{-2}$  nC. The jet charge is several orders of magnitude smaller than the total charge on the electrode. The electrode design and target voltage have more effect on the electric field distribution in the space than the jets. The jet charge differences for the different conditions were not significant. The electrostatic charge density on the jet varied a little but the exact charge distribution is unknown. An approximate analysis for the electrostatic field distribution calculation neglects the presence of the jet itself to simplify the analysis. Therefore, in a charge-free region of space, the field is governed by Laplace's equation as given in Equation 4

$$\nabla^2 \varphi = 0 \quad (4)$$

The electric field strength  $E$  was calculated by

$$E = -\nabla \varphi \quad (5)$$

The boundary conditions were as follows: the square plane for collection was grounded, and each needle and the shield ring were set at the same potential.

### 3 EXPERIMENTAL SETUP

The schematic illustrations of the experimental setups used in this study are shown in Figure 2. The polymer solution was forced through a syringe pump through a 2 mm inner diameter silicone rubber tube, resulting in formation of drops of polymer solution at the needle tips when using the 7 needle and the 19 needle systems. When using a 37 needle system, the polymer solution was forced by the syringe pump with a syringe full of air through a reservoir holding PEO solution through a 2 mm inner diameter silicone rubber tube, resulting in the formation of drops of polymer solution at needle tips as shown in Figure 2a. Needles used in all the tests have 0.55 mm inside and 0.6 mm outside diameters.

The needle distribution is shown in Figure 2b and Figure 2c. 4 needle positions are labeled in Figure 2d as 0, 1, 2, 3. Dashed lines are used to show the needles at the same position in this spinneret. The 7 needle system was distributed as position 0 and position 1 needles combined together as shown in Figure 2d and Figure 3a. The 19 needle system was distributed as position 0, 1, and 2 needles combined together as shown in Figure 2b and Figure 2c. The 37 needle system was distributed as position 0, 1, 2 and 3 needles combined together as shown in Figure 2d and Figure 4a. The distance between the adjacent needles was 1 cm. A shield ring, ranging from 7 cm to 10.5 cm diameter, was concentrically fastened with the needles as shown in Figure 2b. The surface smooth shield ring was made with a 0.3 mm diameter iron wire. The shield ring was placed at the same height as the needle tips. The needles and the shield ring were linked with a copper wire connected to the power supply. 6 % (g/ml) PEO ( $M_w=500,000$ ) aqueous solution was used in the

test. The solution viscosity was 763 mPa.s and the solution conductivity was 40  $\mu$ S/cm. The electrospun fibers were collected on a flat 30 cm  $\times$  30 cm grounded target. The distance between the tips of the needles and target was varied from 25 cm to 38.5 cm. The solution was prepared and all experiments were performed at about 25  $^{\circ}$ C in air at 40 % - 60 % RH.

The electrospun fibers were observed with a scanning electron microscope (SEM) (JSM-5910LV, Japan). The IMAGEJ image analysis software was used to determine the fiber diameters. The segments shown in the images are parts of very long fibers. Diameters were measured for about 300 fiber segments per needle as shown in Figures 6-9 in this paper.

The 3D electric fields were calculated by Ansoft Maxwell software using the finite element method. The diameter of the needle was set to 0.6 mm in a cylindrical geometry. To avoid the discontinuity on the edge of the cylinder, it is necessary to chamfer the edges. The radius of the chamfered edge was set to 0.06 mm. The diameter of the shield ring was changed from 5 cm to 14 cm in order to find the optimized shield ring diameter.

## 4 EXPERIMENTAL RESULTS AND DISCUSSION

### 4.1 SIMULATION RESULTS

The 7 needle system is used as an example in this section to show the simulation details as it is the simplest distribution for the hexagon structure. The electric field simulation was done by Ansoft Maxwell software for 3D models in order to find a suitable shield ring diameter.

As the multi-needle setup is a centrosymmetric structure as shown in Figure 3a, only the electric field distribution in the x-z ( $y=0$ ) plane is shown in Figure 3b without a ring shield and Figure 3c with a ring shield. The arrows indicate the direction of the electric field lines with the arrow length proportional to the base 10 logarithm of the electric field strength. The detailed simulation electric field strengths near the tips of the needles and the electric field 5 mm below the needles are also shown in Figure 3d and listed in Table 1.

The results show that the 5 cm ring at 250 mm height shielded the outside needles too much which makes the electric field strength difference  $\Delta E$ ,  $E_0-E_1$ , between the nozzle of the position 0 needle and the position 1 needles to be  $2.2 \times 10^6$  V/m at the tip of the needle; while a 9 cm ring cannot shield the position 1 needles enough which makes the electric field strength difference  $\Delta E$  between the tip of the position 0 needle and the position 1 needles to be  $-1.9 \times 10^6$  V/m at the tip of the needle. The electric field strength difference  $\Delta E$  between the tip of the position 0 needle and the position 1 needles with a 7 cm ring is  $-1.5 \times 10^6$  V/m.

The 5 cm shield ring makes the electric field strength difference  $\Delta E$  between the tip of the position 0 needle and the position 1 needles to be  $2 \times 10^4$  V/m at 245 mm which is 5 mm below the needles; while a 9 cm shield ring cannot shield the outside needles enough which makes the electric field strength difference  $\Delta E$  between the tip of the position 0 needle and the position 1 needles to be  $-5 \times 10^4$  V/m at 245 mm. The electric field strength difference  $\Delta E$  between the tip

of the position 0 needle and the position 1 needles with a 7 cm ring is  $-3 \times 10^4$  V/m at 245 mm.

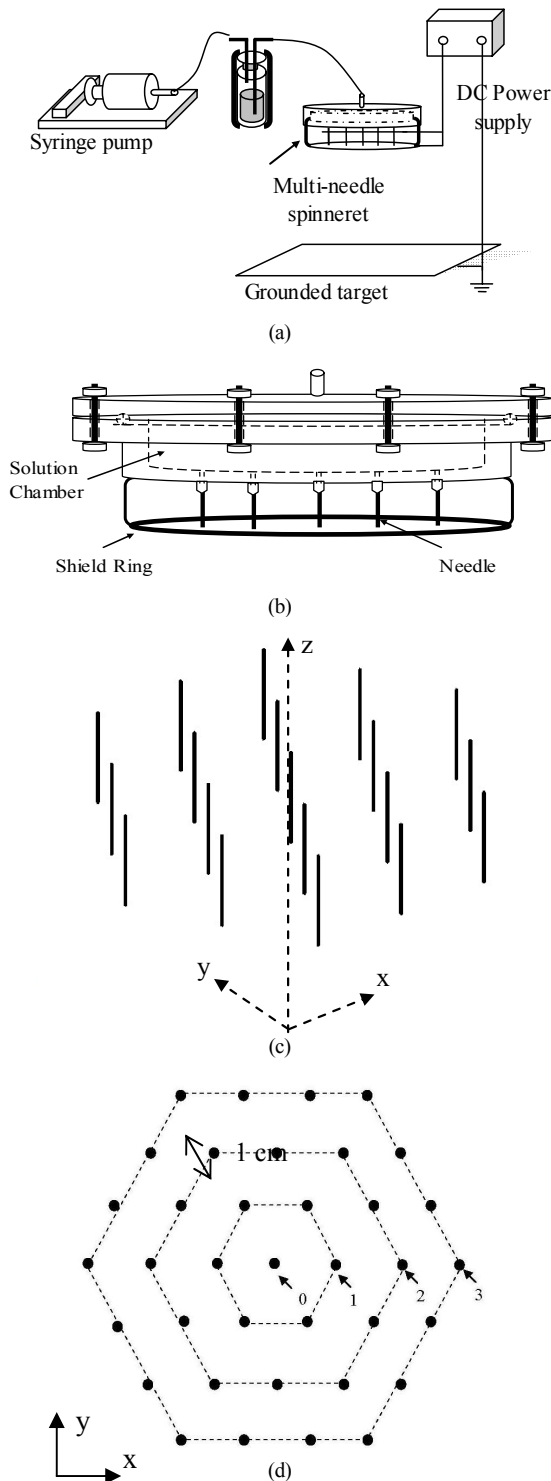


**Figure 2.** (a) The schematic illustration of the electrospinning setup; (b) The details of the spinneret with a shield ring; (c) 3D 19 needle spinneret illustration; (d) The 2D needle distributions in the x-y plane for a single needle (position 0) plus hexagon needle arrays for 7 (positions 0 and 1), 19 (positions 0, 1, and 2), and 37 (positions 0, 1, 2, and 3) needle systems.

The angle away from the z axis was defined as the angle between the vertical axis and the electric field line. The angle shown in Table 1 is the angle just below the

needles from the axis of the cylindrical needles. The simulation results at 245 mm height also show that the angle away from the z axis is  $23^\circ$  without the shield ring,  $17^\circ$  with a 9 cm shield ring,  $9.4^\circ$  with a 7 cm shield ring,  $7^\circ$  with a 5 cm shield ring 5 mm below the tip of the needle. The electric field is more focused with a smaller shield ring.

Based on the discussion above and the comparison in Figure 3d, the 7 cm shield ring was used as a trade off to get a relatively more uniform and at the same time more focused electric field.

**Table 1.** Calculated electric field strength and direction for the 7 needle system. All needle tips and the ring shield were 25 cm above the ground target

Ring Diameter	Height	Needle position	E (V/m)	Angle away from the z axis ( $^\circ$ ) ***
5 cm*	250 mm	0	$5.4 \times 10^6$	0
		1	$3.2 \times 10^6$	0
	245 mm	0	$4.0 \times 10^5$	0
7 cm*	250 mm	1	$3.8 \times 10^5$	7
		0	$5.2 \times 10^6$	0
	245 mm	0	$3.0 \times 10^5$	0
9 cm*	250 mm	1	$3.3 \times 10^5$	9.4
		0	$5.3 \times 10^6$	0
	245 mm	0	$3.0 \times 10^5$	0
No ring**	250 mm	1	$3.5 \times 10^5$	17
		0	$1.1 \times 10^7$	0
	245 mm	0	$1.3 \times 10^7$	0
		0	$5.6 \times 10^5$	0
		1	$6 \times 10^5$	23

\*the reference voltage was set to 25 kV with shield ring system;

\*\* The reference voltage was set to 22.5 kV without the ring.

\*\*\* Angle away from the z axis means the angle between the vertical Z axis and the electric field line.

The equilateral triangle distribution can be iterated endlessly, keeping the distance between nearest needles the same. The 19 needle and 37 needle systems were also tested.

The shield ring diameter in the 37 needle system was chosen following the same rules as the 7 needle system. Different shield ring diameters with 8 cm, 10.5 cm and 14 cm were simulated in order to make  $\Delta E$  in the range of 0 to 5 mm below the needle tips smaller. The simulation results also show that the 8 cm ring at 300 mm height shielded the outside needles too much; while a 14 cm ring can not shield the position 3 needles enough. So, a 10.5 cm diameter shield ring was used and is discussed in detail below.

The simulation electric field strengths for the 37 needles system near the tips of the needles and the electric field 5 mm below the needles with a 10.5 shield ring and without the shield ring are shown in Figure 4 and listed in Table 2. The results show that with the 10.5 cm shield ring, the largest electric field strength difference  $\Delta E$  between the position 3 needles and position 0 needle is  $2.4 \times 10^6$  V/m at the needle tips 300 mm above the grounded target. The largest electric field strength difference  $\Delta E$  between the position 0 needle and the position 2 needles at 295 mm is  $3 \times 10^4$  V/m which is 5 mm below the needle tips. The 37 needle system with the 10.5 cm shield ring was used in tests. The difference between

the position 3 needles and the position 0 needle  $\Delta E$  was  $3 \times 10^6$  V/m in the system without the shield ring at 300 mm height. The electric field strength difference  $\Delta E$  between the position 3 needles and the position 0 needle is  $8 \times 10^4$  V/m at 295 mm which is 5 mm below the needle tips.

At 300 mm height with a ring shield system, the electric field strength of position 1 needles was larger than the electric field strength of position 0 needle and the electric field strength of position 2 needles was larger than the electric field strength of position 1 needles. The electric field strength of position 2 needles was smaller than the electric field strength of position 3 needles with both systems. Similar tendency was found in 37 needles system without the shield ring. This means that outside needles shielded the electric field inside which can make the electric field at the inside tips more uniform.

Without the shield ring 5 mm below the tips of the needles, the angles away from the z axis changed from 0 to  $29^\circ$  while the angles away from the z axis changed from 0 to  $17^\circ$  with the shield ring. The angle of position 1 needles was smaller than the angle of position 2 needles and the angle of position 2 needles was smaller than the angle of position 3 needles. Based on this result, the outside needles can also help to focus the electric field just as the shield ring does. The shield ring can focus the electric field and make it more uniform in the 37 needle system.

## 4.2 EXPERIMENTAL DEMONSTRATION

Based on the simulation results, some experiments were performed to demonstrate the robust multi-needle electrospinning spinneret design. The electrospun mats are shown in Figure 5.

The experiments with 7 needles were tested first. The stable spinning with 7 jets lasts about 1 hour but it can be easily disturbed by random factors such as one of the jets stopped spinning without the shield ring. With the 7 cm shield ring, the process can be stable for as long as 4 hours.

Figures 6 and 7 show the SEM results of electrospun fibers and the fiber diameter distributions with PEO-water solutions at different positions of the 7 needle system. The distributions of the fiber diameters ranged from 200 nm to 600 nm and the mean diameters were all about 400 nm at 22.5 kV without the shield ring; the distributions of the fiber diameters ranged from 300 nm to 500 nm and the mean diameters were all about 400 nm at 25 kV with the shield ring. The distribution of fiber diameters with a 7 cm diameter shield ring was narrower than that with the 7 needle system without the shield ring.

As mentioned in Section 2, larger electric field strength needs a larger injection rate for the outside needles so the solution rate from the pump doesn't match the output of the outside needles. This is the reason for the larger distribution of the fibers from the position 1 needles in the fiber collection which makes the process sensitive to disturbances.

The distributions of the fiber diameters of the shield ring system were almost the same with the distributions of the fiber diameters of the single needle system as shown in our previous work [16]. It should be noted that smaller fibers could also be produced in the shield ring system with smaller electric field strength at the tip but larger average  $E$  in the working distance between needle tips and the grounded target.

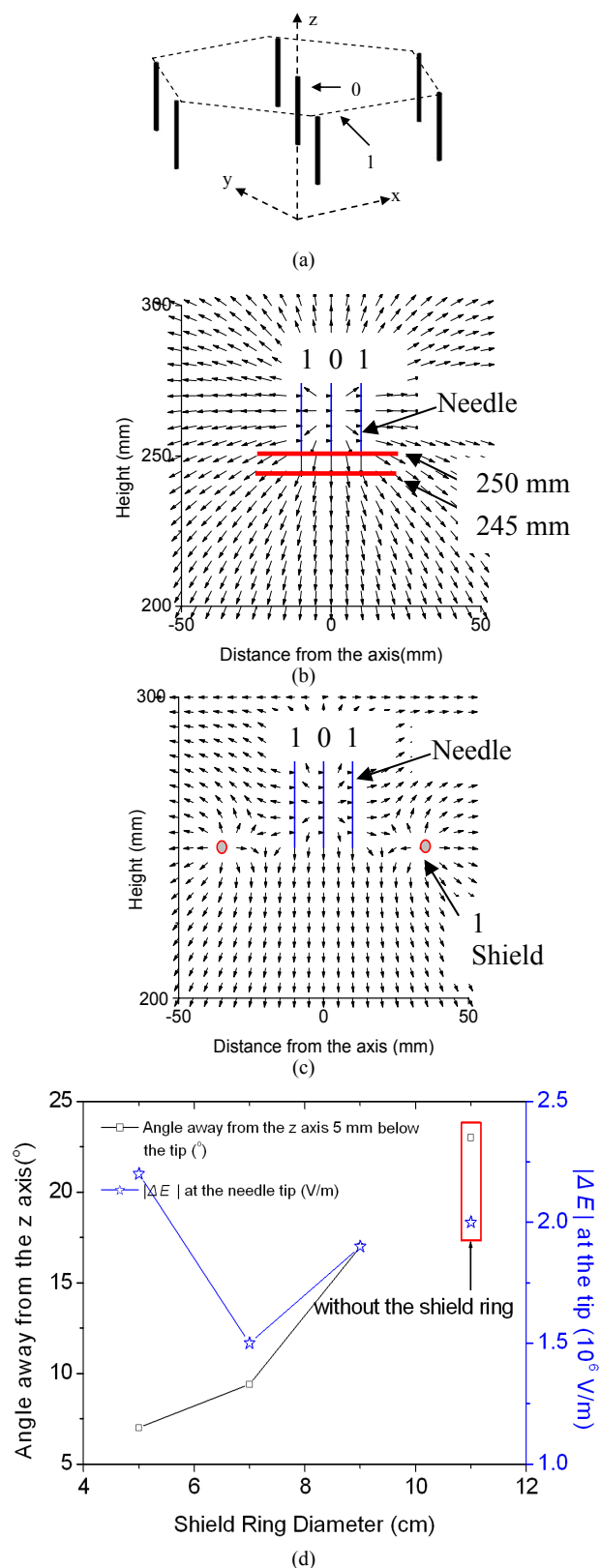


**Figure 3.** (a) The 3D schematic illustration of the experimental 7 needle spinneret with needle tips 250 mm above the grounded target; calculated electric field distribution of the 7 needle system (b) without a shield ring; (c) with a 7 cm diameter shield ring system; (d) The relationship between the shield ring diameter, the electric field angle away from the z axis and absolute value of the electric field difference between position 0 and position 1 needles.



The diameter of the fiber collection is 15 cm and the boundaries of the small mats were clear with the 7 needle system without the shield ring as shown in Figure 5a. The diameter of the fiber collection is 12 cm and the boundaries of the small mats disappeared in the shield ring system causing a more uniform and more focused electric field as shown in Figure 5b. The electric field distribution can affect the jet path which was demonstrated in our previous work [17, 19] by high speed camera. As shown in Table 1, the angle of the electric field line away from the vertical axis near the tip of the needle was smaller with the shield ring than without the shield ring. The electric field modified by the shield ring was more focused which can help to produce fibers in a smaller collection area.

**Table 2.** Calculated electric field strength and direction of the 37 needle system. All needle tips and the ring shield were 30 cm above the ground target

Ring Diameter	Height (mm)	Needle position	E (V/m)	Angle away from the z axis (°) ***
No ring*	300	3	$7.9 \times 10^6$	0
		2	$6.5 \times 10^6$	0
		1	$4.9 \times 10^6$	0
		0	$4.9 \times 10^6$	0
		3	$5.2 \times 10^5$	29
	295	2	$4.9 \times 10^5$	15
		1	$4.6 \times 10^5$	5
		0	$4.4 \times 10^5$	0
	10.5 cm shield Ring system**	3	$6.9 \times 10^6$	0
		2	$5.3 \times 10^6$	0
		1	$5.1 \times 10^6$	0
		0	$4.5 \times 10^6$	0
		3	$4.9 \times 10^5$	17
	295	2	$5.0 \times 10^5$	9
		1	$4.7 \times 10^5$	3
		0	$4.7 \times 10^5$	0

\*The simulation voltage was set to 30 kV without the shield ring;

\*\* the simulation voltage was set to 50 kV with the 10.5 cm shield ring.

\*\*\* Angle away from the z axis means the angle between the vertical z axis and the electric field line.

The 19 needle system and 37 needle system were also tested in the experiments. The electrospun mats from the 19 needle system are shown in Figure 5c and 5d. The electrospun mats from the 37 needle system are shown in Figure 5e and 5f. The 37 needle systems are used as an example in the following discussion.

The boundaries of the 37 round mats are clear at the beginning but disappear after about 1 hour. The spinning process is stable for more than 4 hours with the shield ring and is insensitive to random disturbances. However, the output mass of the position 4 needles are larger than input mass which sometimes causes jet discontinuity when the spinning lasts for a long time as the electric field distribution is not uniform without the ring.

Figure 8 without a ring shield and Figure 9 with a ring shield show the SEM results of electrospun fibers and the fiber diameter distributions with PEO-water solution at different positions. The results show that the fiber diameter distributions are almost the same although the needle positions are different. The distributions of the fiber diameters all range from about 200 nm to 450 nm. The mean diameters of the two systems at different conditions

are all about 300 nm as shown in Figures 8 and 9. There is no obvious difference in fiber diameter distributions between the two systems when using the 37 needle system.

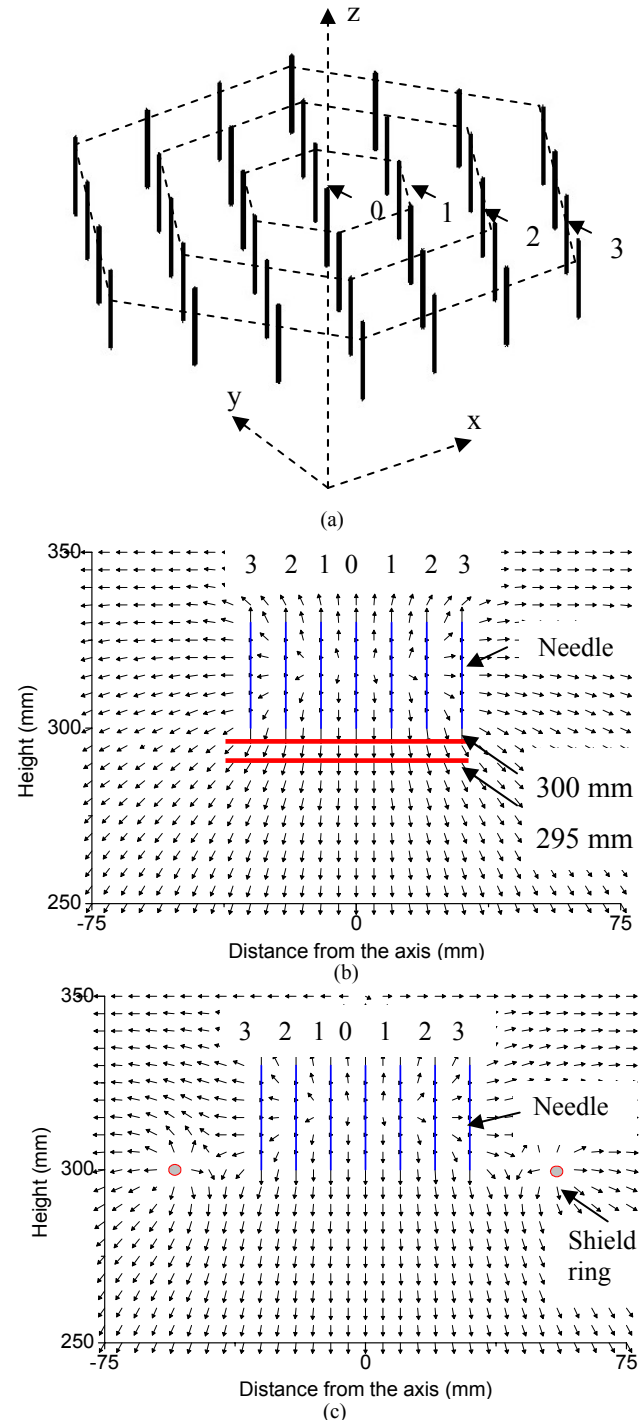


**Figure 4.** (a) The 3D schematic illustrations of the experimental 37 needle spinneret with needle tips 300 mm above the grounded target; Calculated electric field distribution of the 37 needle system (b) without a shield ring and (c) with a 10.5 cm diameter shield ring system.

It should be mentioned that when the number of the needles increased from 1 to 37, the fiber diameters greatly decreased from 400 nm-670 nm with single needle [19] to 200 nm- 450 nm although the solution rate increased from 0.1 ml/h to 0.5 ml/h. The increased number of needles makes the electrode act more like a plate electrode which

could yield a smaller electric field strength at the needle tips with larger average electric field strength in the working space which is defined as the applied voltage on the needles divided by the distance from the needle to the grounded target. The relationship is shown in Figure 10. Our previous work in [18] shows that a higher voltage at the nozzle can produce a larger average electric field strength which will help produce smaller fiber diameters for the large bending frequency. This is also proved by the testing multi-needle systems.

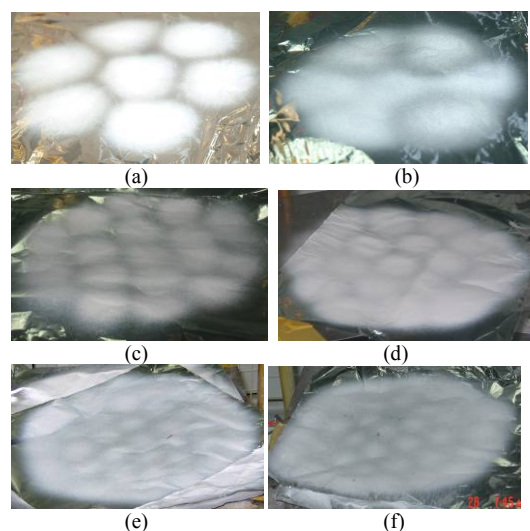


**Figure 5.** Fiber mats collected on the target with the multi-needle systems (a) Electrospinning with the 7 needle system at 22.5 kV, flow rate 0.7ml/h, distance between the needle tips and the target 25 cm, without a shield ring; (b) Electrospinning with a 7 needle system at 25 kV, flow rate 0.7ml/h, distance between the needle tips and the target 25 cm and shield ring diameter 7 cm; (c) Electrospinning with 19 needle system at 28.5 kV, flow rate 2.9 ml/h, distance between the needle tips and the target 30 cm; (d) Electrospinning with 19 needle system at 43 kV, flow rate 2.9ml/h, distance between the needle tips and the target 30 cm with a 9 cm shield ring; (e) Electrospinning with 37 needle system at 57.5 kV, flow rate 18.5 ml/h, distance between the needle tips and the target 38.5 cm with a 10.5 cm diameter shield ring and (f) at 46.8 kV, flow rate 6 ml/h, distance between the needle tips and the target 35 cm without a shield ring.

The working distance between the tips of the needles and the target increase when increasing the number of needles. For a single needle system, 15 cm is the shortest working distance between needle tips and the grounded target for 0.1 ml/h solution rate [19]; for the 7 needle system 25 cm is the shortest working distance for 0.1 ml/h per needle; for the 19 needle system the shortest working distance is 30 cm for 0.15 ml/h per needle; and for the 37 needle system the shortest working distance is 35-38.5 cm for 0.5 ml/h per needle.

Based on the calculation and discussion in our previous work [18], the growing spiral electrospinning jet path subtending a bending angle is related to the electric field direction with slope  $E_z(x,z)/E_x(x,z)$ .

The more uniform the electric field is, the smaller the bending angle is. The increased number of needles makes the electrode act more like a plate electrode and makes the field more uniform. We believe that more needles cause smaller bending angles due to the smaller electric field slope as shown in Figure 4b. This was confirmed by Yarin group using high speed camera in their system [6]. Smaller bending angles

could decrease the total evaporation rate. This may be one of the reasons for the larger working distance needed when using a larger number of needles. At the same time, a large number of jets require more solvent evaporation space than a single jet.

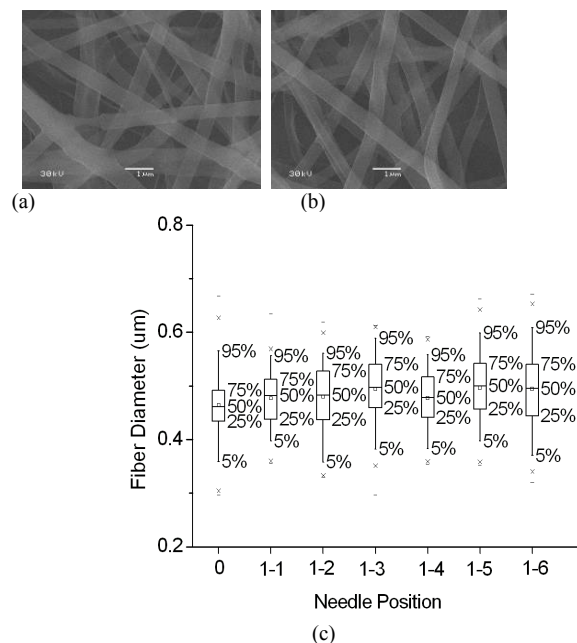


**Figure 6.** Electrospinning fibers with a 7 needle system without a shield ring, 0.7ml/h, 25 cm height needle tips at 22.5 kV (a) SEM result of the mat from position 0 needle in the middle; (b) SEM result of the outside 6 mats from position 1 needles; (c) Electrospinning fiber diameter distribution with PEO-water solution. 1-x(x from 1 to 6) means the position x needle in position 1 needles. In this paper, the values represented are the 5<sup>th</sup> percentile, 25<sup>th</sup> percentile, median, 75<sup>th</sup> percentile, and 95<sup>th</sup> percentile of the fiber diameter distribution[21]. For each needle approximately 300 fiber segments were measured for diameters by ImageJ.

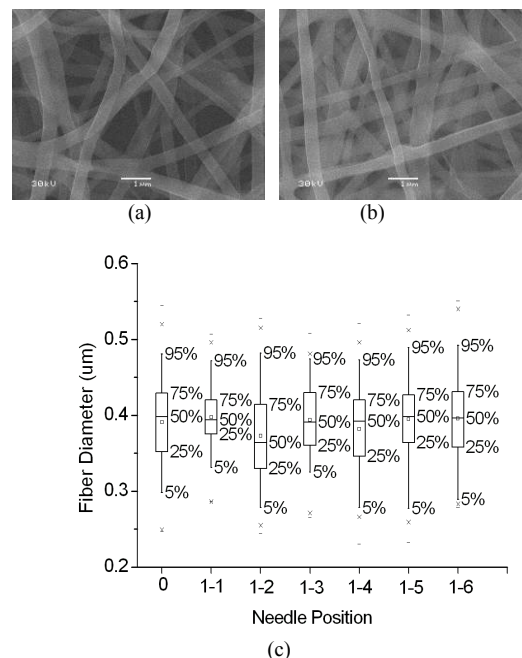


**Figure 7.** Electrospinning fibers with a 7 needle system with a 7 cm diameter shield ring at 25 kV, 0.7ml/h, and 25 cm height of needle tips (a) SEM result of the mat from position 0 needle in the middle; (b) SEM result of the outside mats from position 1 needles; (c) Electrospinning fiber diameter distribution with PEO-water solution. 1-x(x from 1 to 6) means the position x needle in position 1 needles.



## 5 CONCLUSION

A novel hexagon-distributed multi-needle spinneret was designed and tested. A robust multi-needle electrospinning process can be achieved with a suitable shield ring design based on the electric field simulation results. It was found that thinner fibers can be produced with the shield ring system because of the more uniform electric field near the tips of the needles and because of the larger average electric field strength in the fiber formation space. It was demonstrated that the more needles used, a larger space was needed for jet stretching. This design and the results provide a useful concept to scale up multi-needle electrospinning processes.

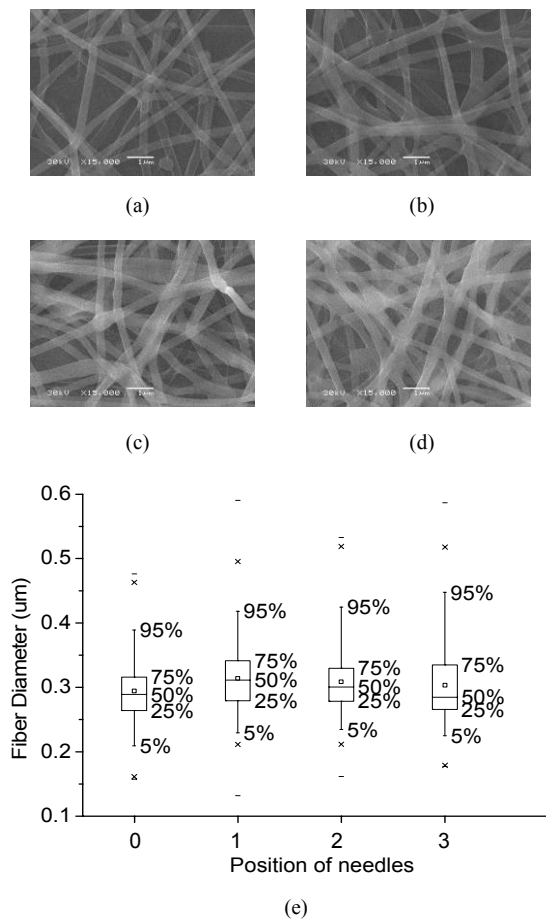


**Figure 8.** SEM results of electrospinning fibers with a 37 needle system without a ring at 46.8 kV, 6 ml/h, 35 cm height of needle tips (a) Fibers from position 0 needle; (b) Fibers from position 1 needles; (c) Fibers from position 2 needles; (d) Fibers from Position 3 needles; (e) Fiber diameter distribution with PEO-water solution.

## ACKNOWLEDGEMENTS

The authors would also like to thank Mr. Matthew Mannarino for his contributions to proofreading the paper for English and grammar. The work was supported by Grant No. 50677032 from the National Natural Science Foundation of China, supported by grants from Specialized Research Fund for the Doctoral Program of Higher Education (SRFDP) (20060003029) and supported by 2006 DEIS graduate fellowships.

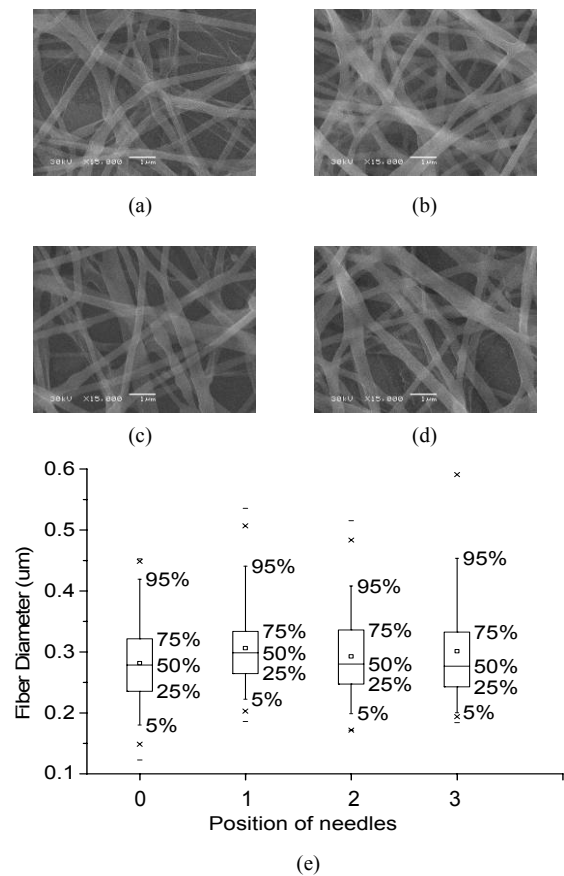


**Figure 9.** SEM results of electrospinning fibers with a 37 needle system with a 10.5 cm diameter shield ring at 57.5 kV, 18.5 ml/h, 38.5 cm height of needle tips and ring shield (a) Fibers from position 0 needle in the middle of the needles; (b) Fibers from position 1 needles; (c) Fibers from position 2 needles; (d) Fibers from position 3 needles; (e) Electrospinning fiber diameter distribution with PEO-water solution.

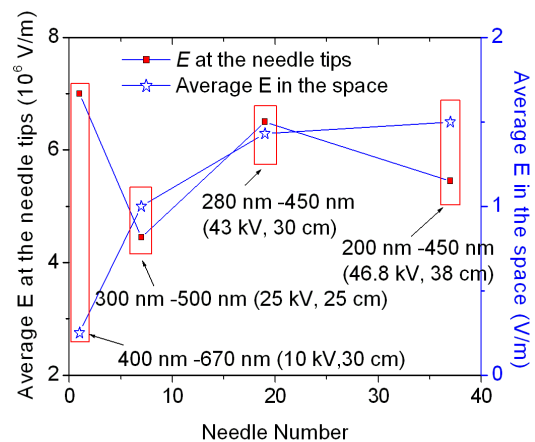


**Figure 10** The calculated relationship between the needle number and average electric field strength at the needle tips and average E in the working space. The single needle experiments did not require a shield ring, but the 7, 19 and 37 needle experiments had a shield ring. Each pair of electric field data points have the fiber diameter range, needle voltage, and needle height given.

## REFERENCES

- [1] P. P. Tsai, H. Schreuder-Gibson, and P. Gibson, "Different electrostatic methods for making electret filters", *J. Electrostat.*, Vol. 54, pp. 333, 2002.
- [2] Z. M. Huang, Y.Z. Zhang, M. Kotaki, S. Ramakrishna, "A review on polymer nanofibers by electrospinning and their applications in nanocomposites", *Composites Sci. Techn.*, Vol. 63, pp. 2223-2253, 2003.
- [3] D. Li, J. T. McCann, and Y. Xia, "Use of electrospinning to directly fabricate hollow nanofibers with functionalized inner and outer surfaces", *Small*, Vol. 1, No. 1, pp. 83-86, 2005.
- [4] A. L. Yarin, E. Zussman, "Upward needleless electrospinning of multiple nanofibers", *Polymer*, Vol. 45, pp. 2977-2980, 2004.
- [5] O. O. Dosunmu, G. G. Chase, W. Kataphinan and D. H. Reneker, "Electrospinning of polymer nanofibers from multiple jets on a porous tubular surface", *Nanotechnology*, Vol. 17, pp. 1123-1127, 2006.
- [6] D. Lukas, A. Sarkar, and P. Pokorny, "Self-organization of jets in electrospinning from free liquid surface: A generalized approach", *J. Appl. Phys.*, Vol. 103, 084309, 2008.
- [7] T. Miloh, B. Spivak and A. L. Yarin, "Needleless electrospinning: Electrically driven instability and multiple jetting from the free surface of a spherical liquid layer", *J. Appl. Phys.*, 106, 114910, 2009.
- [8] S. A. Theron, A. L. Yarin, E. Zussman, and E. Kroll, "Multiple jets in electrospinning: experiment and modeling", *Polymer*, Vol. 46, pp. 2889-2899, 2005.
- [9] W. Tomaszewski, M. Szadkowski, "Investigation of electrospinning with the use of a multi-jet electrospinning head", *Fibers Textiles in Eastern Europe*, Vol. 13, No. 4, pp. 22-26, 2005.
- [10] G. H. Kim, Y. S. Cho and W. D. Kim, "Stability analysis for multi-jets electrospinning process modified with a cylindrical electrode", *European Polymer J.*, Vol. 42, pp. 2031-2038, 2006.
- [11] Y. Yang, Z. D. Jia, Q. Li, H. F. Gao, and Z. C. Guan, "The study on multiple needles electrospinning systems with uniform nanofibers", *IEEE 8th. Intern. Conf. Properties and Applications of Dielectric Materials*, pp. 26-30, 2006.
- [12] A. Varesano, R. A. Carletto and G. Mazzuchetti, "Experimental investigations on the multi-jet electrospinning process", *J. Materials Processing Technology*, Vol. 209, pp. 5178-5185, 2009.
- [13] C. J. Angammana and S. H. Jayaram, "Effects of Electric Field on the Multi-jet Electrospinning Process and Fiber Morphology", *Electrostatics Joint Conf.*, section 03 (No. 3.4), Boston University, 2009.
- [14] J. M. Deitzel, J. Kleinmeyer, D. Harris, and N. C. B Tan, "The effect of processing variables on the morphology of electrospun nanofibers and textiles", *Polymer*, Vol. 42, pp. 261-272, 2001.
- [15] Y. Yang, Z. D. Jia, L. Hou, Q. Li, L. M. Wang, and Z. C. Guan, "Controlled deposition of electrospinning jet by electric field distribution from an insulating material surrounding the barrel of the polymer solution", *IEEE Trans. Dielectr. Electr. Insul.*, Vol. 15, pp. 269-276, 2008.
- [16] Y. Yang, Z. D. Jia, and Z. C. Guan, "Controlled deposition of electrospun Poly(ethylene oxide) fibers", *IEEE Intern. Conf. Dielectric Liquids*, pp. 457-460, 2005.
- [17] Y. Yang, Z. D. Jia, Q. Li, Z. C. Guan, "Experimental investigation of the governing parameters in the electrospinning of polyethylene oxide solution", *IEEE Trans. Dielectr. Electr. Insul.*, Vol. 13, pp. 580-585, 2006.
- [18] Y. Yang, Z. D. Jia, J. N. Liu, Q. Li, L. Hou, L. M. Wang and Z. C. Guan, "Effect of electric field distribution uniformity on electrospinning", *J. Appl. Phys.*, Vol. 103, 104307, 2008.
- [19] Y. Yang, Z.D. Jia, J.N. Liu, L.M. Wang and Z.C. Guan, "The effects of flow rate and the distance between the nozzle and the target on the operating conditions of electrospinning", *J. Polymer Eng.*, Vol.28 (1-2), pp. 67-86, 2008.
- [20] Y. Yang, Z.D. Jia, Q. Li, J.N. Liu and Z.C. Guan, "Effect of 'Stagnation Plane' in the Electric Field during the Electrospinning Process", *IEEE Trans. Dielectr. Electr. Insul.*, Vol. 16, pp. 409-416, 2009.
- [21] <http://www.originlab.com/index.aspx?s=8&lm=214&pid=959>



**Ying Yang** was born in Hebei province, China in 1981. She received the Ph.D. degree in electrical engineering from Tsinghua University, Beijing, China in 2008 and the B.S. degree in environmental engineering from Tsinghua University, Beijing, China in 2003. Her research interests are electrospinning and its applications.

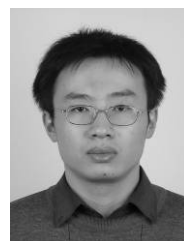


**Zhidong Jia** was born in Taiyuan, China in 1966. He received the B.S and Ph.D. degrees in electrical engineering from Xi'an Jiaotong University, China in 1987 and 2001, respectively. He received the M.S degree in electrical engineering from Tsinghua University in 1992. From 2001 to 2003 he worked as a postdoctoral fellow in Tsinghua University. He is now an associate professor at the Graduate School at Shenzhen, Tsinghua University. His major research fields are high voltage insulation,

improvements on RTV coatings, prevention of ice formation on outdoor insulations, and electrospinning.



**Qiang Li** was born in Beijing, China in 1982. He received the B.S. and M.S. degrees in electrical engineering from Tsinghua University, Beijing, China in 2005 and 2007, respectively. His research interests are electrospinning and its applications.



**Lei Hou** was born in Henan province, China in 1979. He received the B.S. degree in electrical engineering from Huazhong University of Science and Technology, Wuhan, China in 2005. He is a Ph.D. degree candidate in electrical engineering at Tsinghua University, Beijing, China. His research interests are mechanical behavior of outdoor insulation and overhead transmission line and electrospinning.



**Jianan Liu** was born in Guangdong Province, China in 1984. She received the B.S. degree in electrical engineering from Tsinghua University, Beijing, China in 2007. She is now a Masters student in electrical engineering at Tsinghua University, Beijing, China. Her research interests are electrospinning and its applications.



**Liming Wang** was born in Zhejiang Province, China, on 30 November 1963, and received the B.S., M.S., and Ph.D. degrees in high voltage engineering from the Department of Electrical Engineering, Tsinghua University, Beijing, P.R. China, in 1987, 1990, and 1993, respectively. He has worked at Tsinghua University since 1993. His major research fields are high voltage insulation and electrical discharges, flashover mechanisms on contaminated insulators, and applications of pulsed electric fields.



**Zhicheng Guan** was born in Jilin province, China, on 10 November 1944 and received the B.S., M.S., and Ph.D. degrees in high voltage engineering from the Department of Electrical Engineering, Tsinghua University, Beijing, P.R. China, in 1970, 1981, and 1984. He is now Vice President of the Tsinghua University Council and Dean of the Graduate School at Shenzhen, Tsinghua University. His major research fields are high voltage insulation and electrical discharges, and flashover



Markus Zahn (Fellow, IEEE) received the B.S.E.E., M.S.E.E., Electrical Engineer, and Sc.D. degrees from the Department of Electrical Engineering at the Massachusetts Institute of Technology (MIT), Cambridge, MA, in 1968, 1968, 1969, and 1970 respectively. He then joined the Department of Electrical Engineering at the University of Florida, Gainesville until 1980 when he returned to MIT where he is now Professor of Electrical Engineering working in the Research Laboratory of Electronics, Laboratory for Electromagnetic and Electronic

Systems and the High Voltage Research Laboratory. He is also the Director of the MIT Course VI-A EECS Internship Program, a cooperative work/study program with industry. He is the author of *Electromagnetic Field Theory: A Problem Solving Approach* (now out of print) but is working on a new reference book with a complete collection of solved electromagnetism problems. He has also co-developed a set of educational videotapes on demonstrations of electromagnetic fields and energy for the enriched teaching of electromagnetism. He has received numerous excellence in teaching awards at the University of Florida and at MIT. His primary research areas are ferrohydrodynamics and electrohydrodynamics for microfluidic and biomedical applications; nanoparticle technology for improved high voltage performance of electric power apparatus; modeling of electrical streamer initiation and propagation leading to electrical breakdown; Kerr electrooptic field and space charge mapping measurements in high voltage stressed materials, and for the development of model based interdigital dielectrometry and magnetometry sensors for measurement of dielectric permittivity, electrical conductivity, and magnetic permeability with applications to non-destructive testing and evaluation measurements and for identification of landmines and unexploded ordnance. Professor Zahn is co-inventor on 18 patents. He has contributed to about 10 book and encyclopedia chapters, about 115 journal publications, and about 175 conference papers. He is a Fellow of the IEEE; was a Distinguished Visiting Fellow of the Royal Academy of Engineering at the University of Manchester, England; was the 1998 J.B. Whitehead Memorial Lecturer, and was the first James R. Melcher Memorial Lecturer in 2003; is an Associate Editor of the *IEEE Transactions on Dielectrics and Electrical Insulation*; is on the International Scientific Committee on Magnetic Fluids; and has received a Certificate of Achievement for completion of the "Deminers Orientation Course" at the Night Vision and Electronic Sensors Directorate Countermeasures Division at Ft. Belvoir, VA.